Structures 51 (2023) 1328–1340

Contents lists available at ScienceDirect

Structures

journal homepage: www.elsevier.com/locate/structures

Numerical study of steel–concrete composite cellular beam using demountable shear connectors

Xianghe Dai *, Jie Yang, Kan Zhou, Therese Sheehan, Dennis Lam

University of Bradford, Bradford BD7 1DP, UK

ARTICLE INFO

Keywords:
Composite beam
Cellular beam
Demountable shear connector
Numerical modelling
Parametric study

ABSTRACT

Steel concrete composite beams have been increasingly used in practice due to their advantages with respect to their structural features and constructability. However, in conventional composite beam systems composite action is applied via shear connectors welded at the top flange of the down-stand steel beam and embedded in the concrete slabs, making it less favourable for the beam system to be disassembled and reused. This paper presents a numerical study of a new composite beam system consisting of a cellular steel beam, metal deck flooring and demountable shear connectors. According to the experimental study, this composite beam system made the demounting, reassembly, and member reuse possible, and did not compromise the loading capacity. In the numerical study presented in the paper, a finite element model was developed and validated against the results obtained from the previous experimental study. The parametric study further examined the effects of concrete strength, shear connector arrangements and asymmetry ratios of steel beam section to the load capacity of the composite beam system. The analysis and comparison provided a deeper insight into the behaviour of this type of shear connector. Through this numerical study, the structural merits of the composite beam system using demountable shear connectors were highlighted. Finally, the mid-span plastic moment of the composite beam was predicted using the direction method provided in SCI publications and compared with the moment–deflection relationship obtained from FE modelling.

1. Introduction

The building and construction sector is responsible for 39% of global carbon emissions in 2018, 11% of which is from the manufacturing of building materials and products such as steel, cement, and glass [1]. The increasing rate of carbon emission into the environment has highlighted the issue of sustainability and advocated the reuse of materials and intact structural elements. This has led to research on the deconstruction of building structures and reuse of structural members. The steel–concrete composite beam is a cost-effective construction system with competitive behaviour for multi-storey buildings owing to the composite action between the steel beam and composite slab. However, in current construction practice, composite action is mainly achieved through shear studs welded through the profiled sheeting to the steel beam flange and embedded in the concrete slab. When the composite structure reaches the end of its design life, these welded shear connectors make dismantling, adaptation (alteration) and deconstruction almost impossible. Consequently, neither components can be reused straightaway; the concrete slabs have to be crushed, down-cycled or sent to landfill and steel beam has to go through a recycling process. To facilitate reuse, a new form of demountable shear connector is to be used as an alternative to welded connectors in composite beam systems. Unlike welded counterparts, demountable connectors are easy to dismantle, enabling steel beam and concrete slab to be reused with minimum reprocessing and avoiding recycling or crushing processes. In addition, a demountable shear connector can be easily installed into the predrilled holes in beam flange and steel profiled decking on site. Currently this type of demountable shear connector has not been widely adopted in composite beams in practice, and no explicit design guidance is available in addition to the SCI publication P428 [2].

Research on shear connections has been carried out by many researchers [3–21], but only a few investigated the performance of demountable shear connectors. The authors and their research group [22–35] performed a series of push tests, composite beam tests using demountable shear connectors and corresponding numerical modelling and analysis to investigate the structural behaviour and failure modes of demountable shear connectors embedded in concrete slabs and composite beams using demountable shear connectors. The research work

* Corresponding author.
E-mail address: x.dai@bradford.ac.uk (X. Dai).

https://doi.org/10.1016/j.istruc.2023.03.134
Received 29 October 2022; Received in revised form 3 February 2023; Accepted 22 March 2023
Available online 28 March 2023

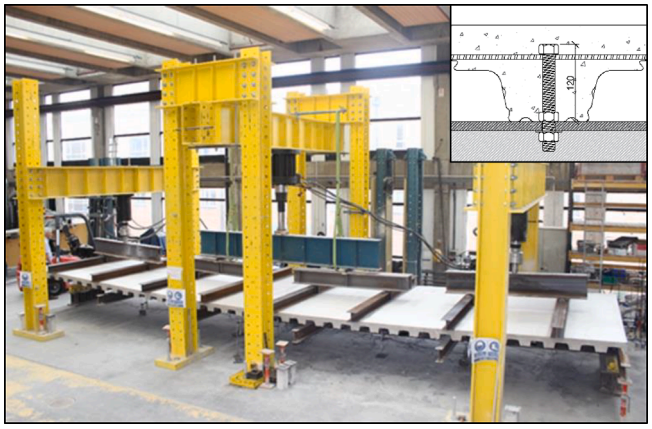

Fig. 1. Test set-up for cellular composite beam.

clearly indicated that the demountable shear connector had very competitive resistance and ductility, the composite beams were easily dismantled and reassembled, therefore previous research studies support the demountable shear connectors to be used as an alternative to welded shear connectors in composite beam systems.

Following an 11.2 m composite cellular beam test carried out at the University of Bradford, an FE model, adopting ABAQUS software and using the concrete damaged plasticity (CDP) material constitutive model, was developed and validated against the experimental results. After the validation of the modelling method, a parametric study, covering different demountable shear connector arrangements, different slab concrete strengths and different asymmetry ratios of steel beam section, was conducted. This paper presents the structural behaviour of the concrete steel cellular beam systems using demountable shear connectors obtained from numerical simulation. The parametric study further highlighted the effects of concrete strength, shear connector arrangement and beam section asymmetry ratio.

2. FE model development and validation

2.1. Test specimen briefing

Before the FE model development, a composite beam consisting of a cellular beam, a concrete slab and demountable shear connection was tested at the University of Bradford. The 11.2 m cellular beam was manufactured from two universal sections. The top T-section was manufactured from Universal Beam 305 × 165 × 46 kg/m S355JR and the bottom T-section came from Universal Column 305 × 305 × 97 kg/m S355J0. The shear connector arrangement (as shown in Fig. 11, CA-0) was a pseudo-elastic distribution with shear connectors in pairs at 300 mm spacing in the outer part, then singly in a staggered pattern at 300 mm spacing (600 mm on each side of the central edge trims) and then at 600 mm in a staggered pattern near the centreline of the beam. Gr. 8.8 M20 bolts were used as the demountable shear connectors as shown in Fig. 1, one nut above the top flange embedded in concrete and another nut tightened/untightened from below. The embedment height of the bolts in concrete was 120 mm (6 times of the diameter) and bolts were tightened to a torque of 120 N·m. Pairs of cast-in edge trims (120 mm in depth) were set in the 150 mm deep composite slab along the beam centreline in the longitudinal axis to facilitate deconstruction. 80 mm deep composite decking (CF80 × 0.9 mm thick) was used. The slab width was 2.8 m (=span/4) for the 11.2 m span. One layer of A193 reinforcing mesh (7 mm wires; 200 mm × 200 mm grid), plus T10 U-bars were placed on top of the metal decking. The use of steel outriggers ('wing' system) was adopted to support the decking so that self-weight and construction loads were applied to the steel beam during casting

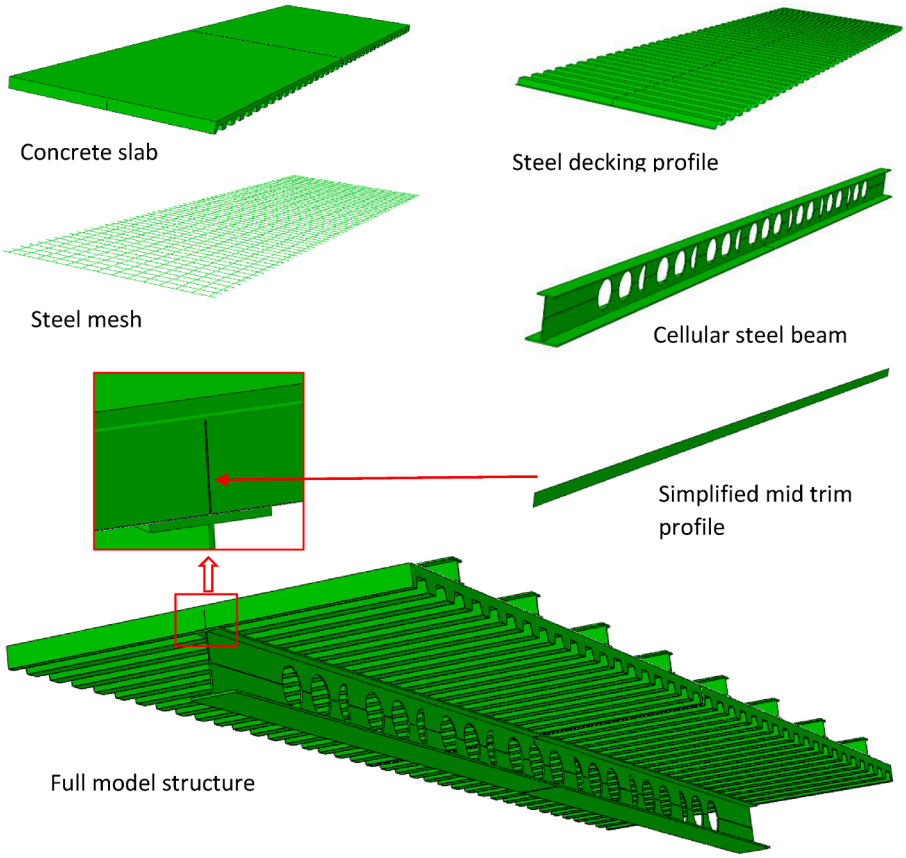

Fig. 2. FE model and assembly of tested composite beam.

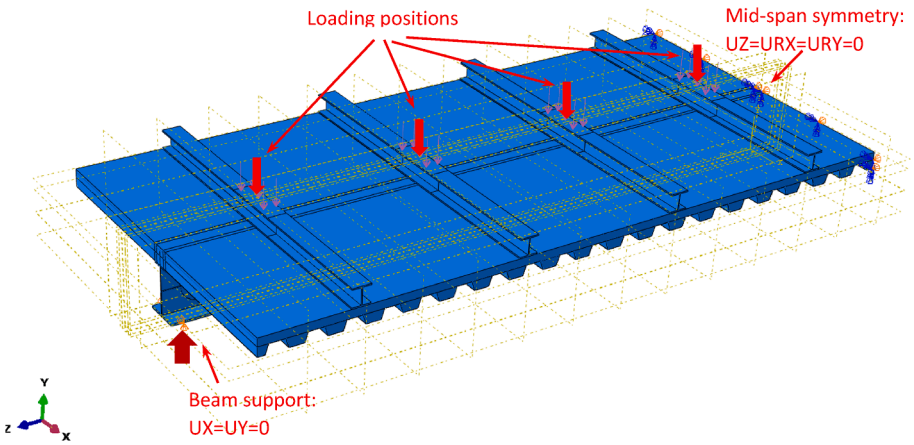

Fig. 3. FE model boundary conditions and loading positions (half of the tested specimen).

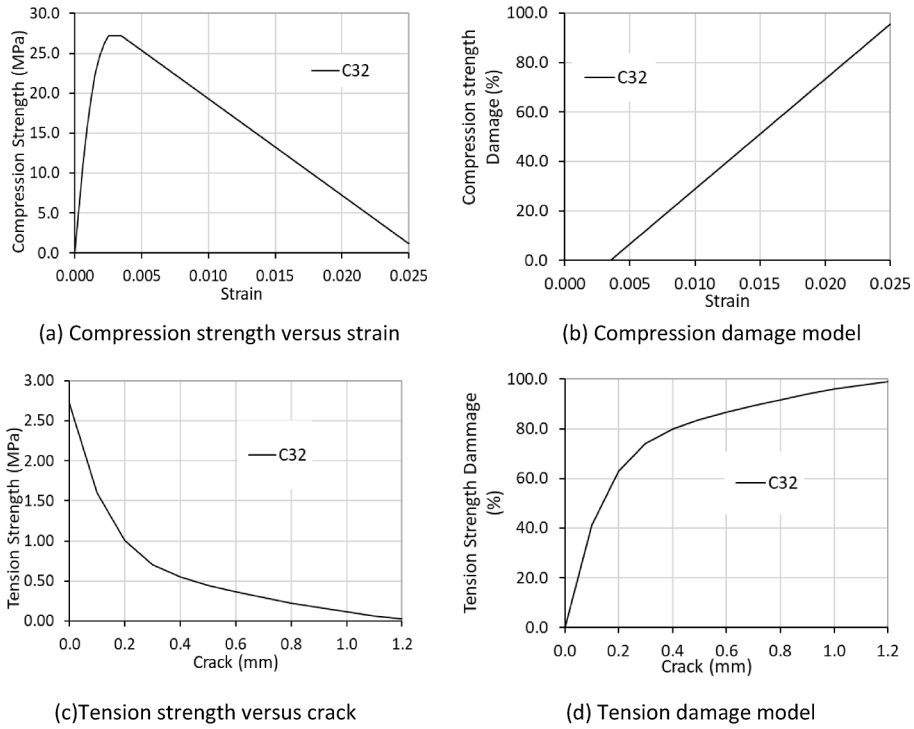

Fig. 4. Concrete compressive and tensile behaviour used for FE model validation.

to simulate an unpropped construction. C30/37 concrete was used with an average test-date cube compressive strength of 39.9 N/mm^2. Fig. 1 shows the composite beam and test set-up at the University of Bradford. The details of the test programme and results are given in reference [34].

The test objectives were to demonstrate long-span cellular composite beams could be designed plastically for a low degree of shear connection using demountable shear connector and also to examine that local composite action could be achieved at the openings to resist Vierendeel bending. The plastic neutral axis of this composite beam was designed to be within the web to a depth of 9 mm. The degree of shear connection was 0.38. The composite beam was designed to fail under bending, with a failure load of 20.7 kN/m^2 plus the self-weight of the beam and slab. The test confirmed this flexural failure mode, with a failure load of 24.1 kN/m^2 and confirmed the design results.

2.2. *Description of the FE model*

The ABAQUS software was employed to develop the FE model and to conduct the numerical simulation. The FE model comprised the cellular steel beam, concrete slab, reinforcement mesh, shear connectors, profiled metal decking and mid edge trims, etc. Considering the symmetrical conditions of the tested specimen across the centre lines of the whole composite beam system, only a half of the specimen was analysed in the simulation to save computational time. The main components of the FE model included the concrete slab, steel decking/trim profiles, cellular steel beam, and reinforced steel mesh. Due to the complication of the shear connection, the shear connectors were modelled by connector elements provided in the ABAQUS software, no substantial solid elements were adopted for shear connector (bolt and nuts). All components were created separately and then assembled to form the composite cellular beam system as the tested composite beam system. Fig. 2 shows the full structural model by mirroring the mid-span plane.

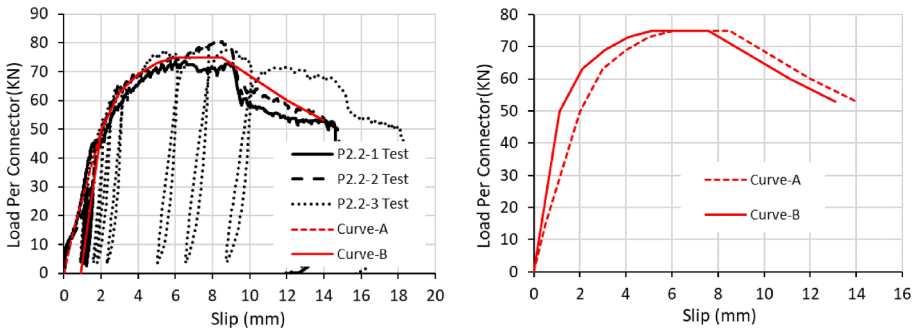

(a) Test curves and average curves (b) Curves with and without initial slip

Fig. 5. Characteristic load-slip behaviour of shear connector obtained from experimental study and used for modelling validation.

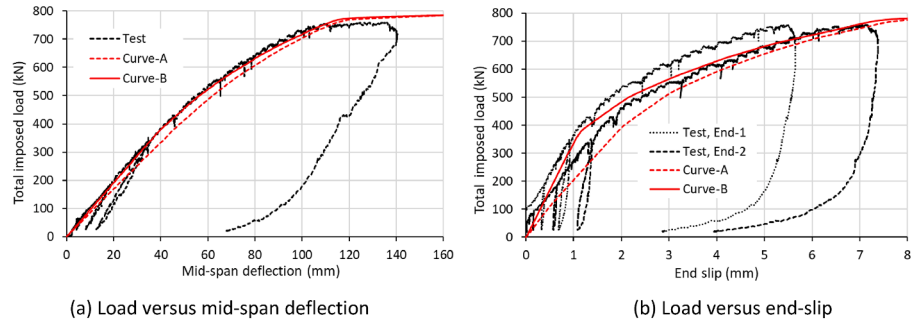

(a) Load versus mid-span deflection (b) Load versus end-slip

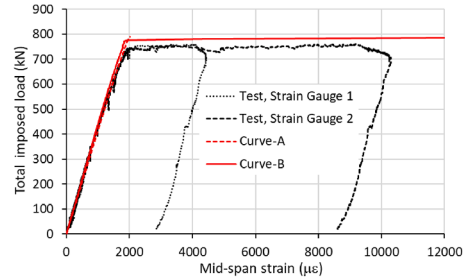

(c) Load versus Strain at bottom flange around the mid-span

Fig. 6. Comparison between FE model prediction and experimental observation.

Three dimensional eight-node solid brick elements with reduced integration (C3D8R) were adopted to mesh the concrete slab, cellular steel beam and load spreader beams. Shell elements (S4R) were used for the metal decking/mid edge trim profiles. Two-node truss/beam elements (T3D2) were used for the reinforced steel mesh. For the main components, a sensitivity study showed that an element size of 75 mm gave the best agreement comparing the prediction with the experimental results and the least computation time required, therefore this mesh size was adopted for this study.

Appropriate contact interactions were defined between different components. Steel mesh reinforcement was embedded into concrete slab to simplify the modelling. The concrete slab and the metal decking profile/mid edge trims were tied. For contact between the decking profile and the steel beam top flange and contact between concrete slab and the mid-edge trim profiles, “hard contact” was assumed for normal behaviour and “penalty” was assumed for the tangential slip behaviour with a friction coefficient of 0.2 adopted. The boundary conditions were defined according to the experimental test set-up. The steel beam at the support points (roller support at bottom flange 100 mm from end) was restrained in the vertical and transverse directions and free in the beam axial direction. To save time, in the FE model, a symmetric boundary condition at the mid-span section was employed: horizontal axial movement and corresponding rotations were restrained. The loads were applied to the load spreader beams in the same manner as for the tested specimen. Fig. 3 shows the FE model boundary conditions and loading positions.

2.3. Steel and concrete material properties

The steel grade of the cellular beam was S355. According to the manufacturer’s specification, the top Tee and bottom Tee had yield strengths of 394 N/mm^2 and 410 N/mm^2, respectively. A Young’s modulus value of 210GPa and a Poisson’s ratio value of 0.3 were used for both Tee sections. For the reinforced steel mesh, yield strength of 500 N/mm^2 with Young’s modulus of 210 GPa and Poisson’s ratio of 0.3 were assumed. The yield strength and the ultimate strength of 450 N/mm^2 were used for metal decking/edge trim profiles according to the manufacturer’s specification. Yield strength of 355 N/mm^2, Young’s modulus of 210GPa and Poisson’s ratio of 0.3 were assumed for the load spreader beams in the modelling.

The specified grade of concrete slab was C30/37. The average compressive cube strength at the test day was 40 N/mm^2 and therefore in the FE modelling, the average concrete cube strength (40 N/mm^2) obtained on the test date was used. The cylinder strength of the concrete

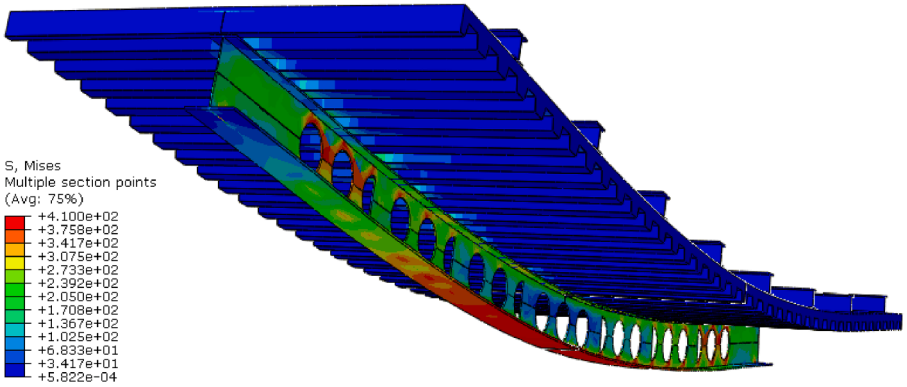

(a) Composite beam deformation and Mises stress distribution

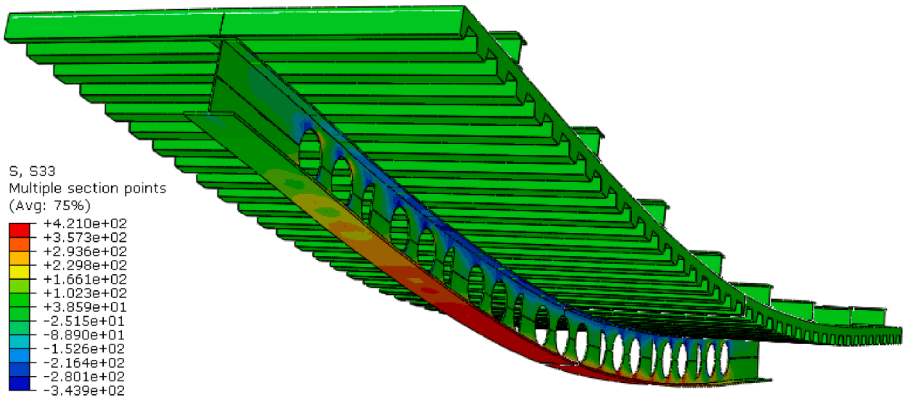

(b) Composite beam axial stress distribution (steel beam top flange under compression, bottom flange under tension)

Fig. 7. Composite beam failure mode and stress distribution by FE model (at mid-span deflection 135 mm).

was taken as 80% of the cube strength, therefore the concrete cylinder strength was 32 N/mm^2. The maximum tensile strength was assumed to be 10% of the maximum compressive strength.

The stress–strain relationships for concrete at high strains were determined according to Eurocode 2 [36] and Eurocode 4 [37]. The maximum design compression strength was taken as the cylinder strength multiplied by a factor of 0.85. Fig. 4 shows the compressive stress–strain relationship, tensile strength-crack width relationship and concrete damage mechanisms under compression and tension, which were adopted in the ABAQUS FE models for the validation.

2.4. Demountable shear connector

Considering the complication of the demountable shear connections, nonlinear fastener/connector element provided in the ABAQUS software was adopted for shear connectors, therefore the shear bolt/nut was not directly modelled in the FE model. The behaviour of the demountable shear connector in the composite cellular beam was determined according to the average load-slip relationship curve obtained from previous push tests at the University of Bradford. As shown in Fig. 5 (a), Curve-A reflected the initial slip and Curve-B started from the second cycle, or the specimen was fully set-up. Fig. 5 (b) compared Curve-A and Curve-B but the initial slip of 0.9 mm in Curve-B was removed. Obviously, the initial slip affects the demountable shear connection stiffness but not the maximum resistance. Ignoring the initial slip for the nonlinear fastener/connector elements in Abaqus may result in a higher stiffness at the initial stage, as shown in Fig. 6(b). The maximum shear capacity was 75.0 kN per shear connector with slippages from 6 mm to 8.5 mm if the initial lip was included.

2.5. FE model validation and comparison/analysis

Fig. 6 compares the predicted behaviours of mid-span deflection vs total imposed load, end slip vs total imposed load and strain at the bottom flange around the mid-span vs total imposed load, against the experimental observations.

Fig. 6 shows the FE predictions successfully captured the main load–deflection, load-end slip behaviour and strain development of the composite cellular steel beam. Using shear connector “Curve-B”, the prediction and experimental observation had satisfactory agreement. This might be explained by the fact that “Curves-B” reflected the shear connector behaviour in the un-propped composite beam system (as the tested specimen) when the initial slip of the shear connector was reduced or eliminated. “Curve-A” might be used for propped composite beam systems or conservative design and calculation of un-propped composite beam systems. Fig. 7 shows the stress distribution of the steel beam and the failure mode. It clearly demonstrates that the steel beam yielded at the bottom of the mid-span. The comparison clearly indicated that the FE model with developed shear connector load-slip behaviour can be used for the simulation of similar composite beam systems and parametric studies.

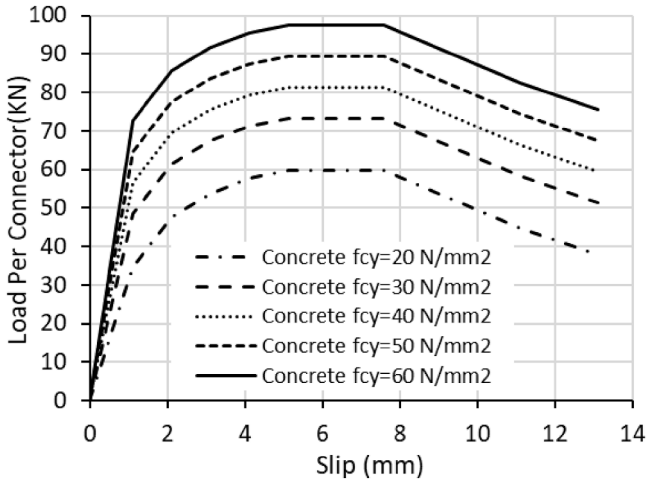

Fig. 8. Assumed characteristic load-slip behaviour of shear connectors with different concrete strength for the parametric study.

3. Parametric study

3.1. Effect of slab concrete strength

To investigate the effect of concrete strength on the composite beam behaviour, a parametric study, considering the change of the concrete strength, was performed. The FE models were based on the tested specimens but different concrete strengths were used. Concrete strength not only affects the slab resistance but also directly affects the shear connector load-slip behaviour, therefore the shear connector behaviours corresponding to different concrete strengths are different. Fig. 8 shows the load to slip relationships of demountable shear connectors using different concretes adopted in this concrete strength parameter study. These relationships are characteristic curves based on shape "Curve-B" in Fig. 5, a benchmark case, with a concrete cylinder strength of 32 N/mm2 and a maximum shear connector resistance of 75 kN/connector at slippages from 6 mm to 8.5 mm before the initial slip of 0.9 mm was removed, based on the demountable shear connector push off tests carried out at the University of Bradford previously, was used to validate a previous FE modelling. The load-slip curves/behaviours for other concrete cylinder strengths (20 N/mm^2 to 60 N/mm^2) were obtained from the validated FE modelling by changing the strengths of concrete. Fig. 9 shows the stress and strain behaviour for the five different concretes adopted in the parametric study, in which the maximum compressive strength in the FE model was the cylinder strength multiplied by a factor of 0.85. Fig. 10 compares the predicted mid-span deflection, end slip and strain at bottom flange vs load relationships of the composite beam systems with different slab concrete strengths. The higher the concrete strength, the higher the load capacity. All five models showed good composite beam performance except the beam with concrete strength C20/25. Due to the lower concrete strength and thus lower shear connector resistance, the shear connection failed when the mid-span deflection reached 132 mm and no steel yielding occurred at the bottom flange (axial strain less than 2000 με).

3.2. Effect of shear connector arrangement

For composite beams, the shear connector plays an important role. It has been recognized that shear connectors close to the end of the composite beam system develop higher shear forces and shear connectors close to the mid-span of the beam system develop lower shear forces. In this parametric study, five different shear connector arrangements, including the arrangement for the tested specimen, along the axial direction of the composite beam system were modelled to examine this effect. Fig. 11 shows the five different shear connector arrangements. Compared with the tested specimen CA-0, in Case CA-a one connector was moved from close to the end to the mid-span, and in Case CA-b a connector was added close to the mid-span. For Case CA-c connectors were fully installed along the beam with 300 mm central spacing in two rows in each trough. For Case CA-d shear connectors were installed with 600 mm central spacing in every second other trough except the first two troughs at the beam ends. Fig. 12 compares the effect of different connector arrangements to the composite beam behaviours. As expected, among these five cases, case CA-c provided the highest overall shear resistance and thus the composite beam system processed the highest load bearing capacity. Although the differences among the cases CA-a, b, c, d are not very evident as the number of connectors adopted are close, it is clear that if the load capacity of the above five composite

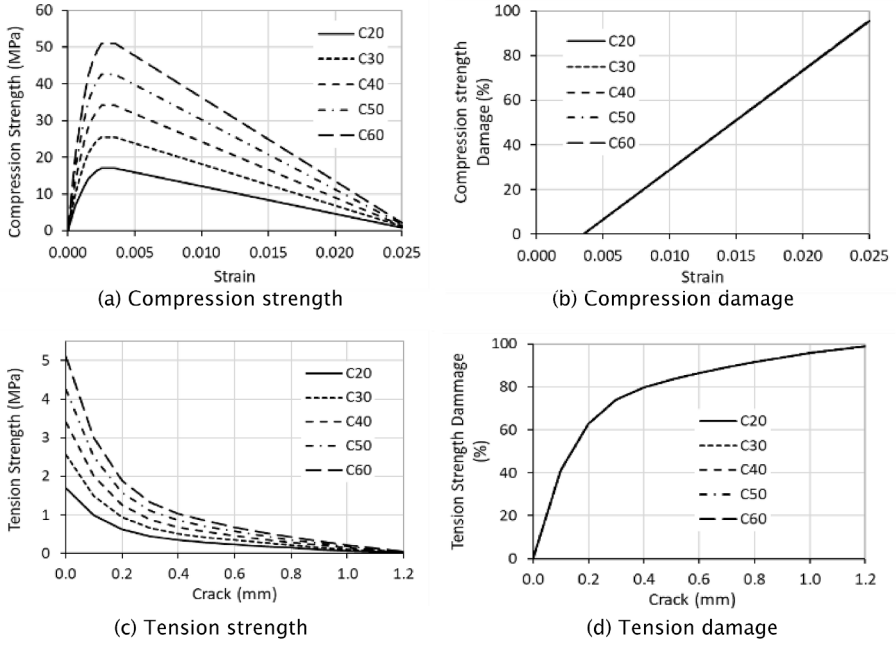

Fig. 9. Five concrete strengths used in the parametric study.

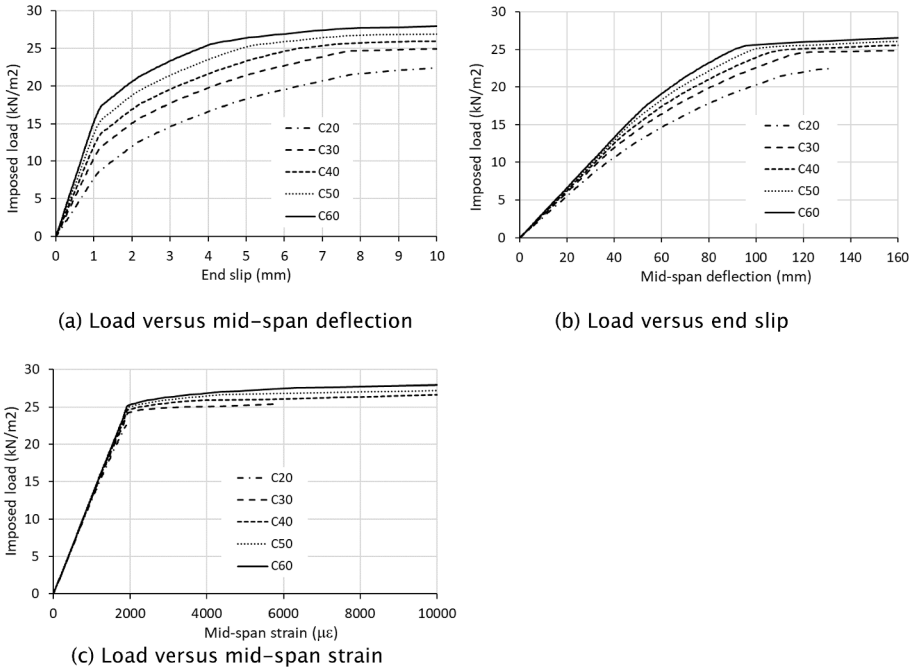

Fig. 10. Effect of slab concrete strengths.

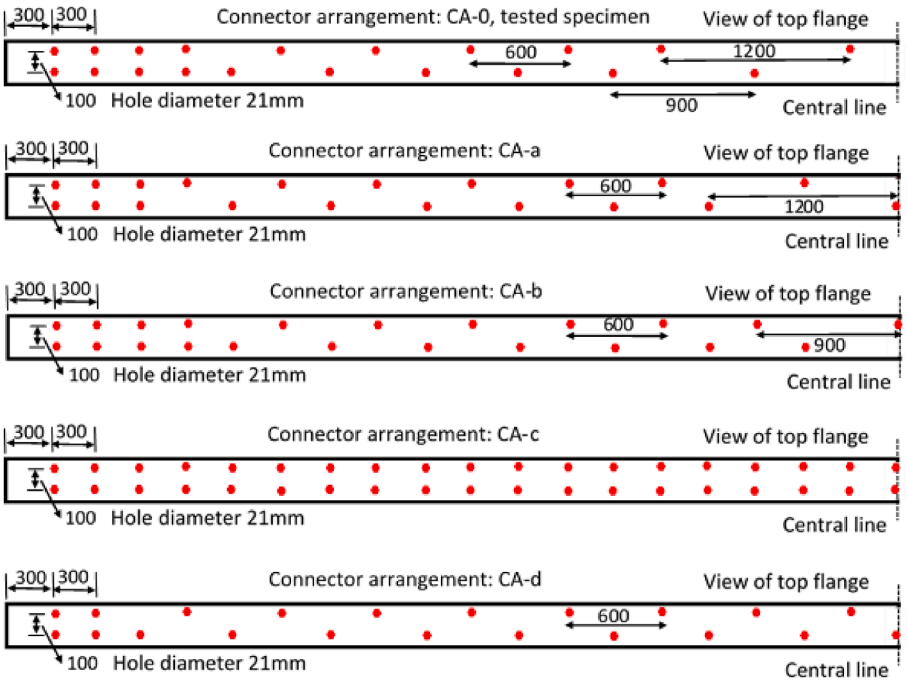

Fig. 11. Five different shear connector arrangements adopted in parametric study.

beam systems were to be ranked, CA-c would come first followed by CA-b, CA-0 (test specimen), CA-a and CA-d with more shear connector reduction at the composite beam ends. Obviously shear connectors close to the ends play an important role in the composite beam system. For flexible shear connector arrangements, pairs of connectors are strongly recommended at high shear regions of the beam that are close to the ends.

3.3. *Effect of ratio of sectional asymmetry*

In order to examine the effect of the ratio of the bottom to top flange areas on the beam system behaviour, based on the tested specimen with the ratio of 2.4 and total cross-sectional area, five other asymmetry ratios from 1.0 to 3.5, by only changing the top flange and bottom flange thickness as shown in Fig. 13, were adopted and all 6 cross sections have same sectional area. The asymmetry ratio is defined as the ratio of the area of bottom flange to the area of the top flange. Fig. 14 compares the effect of different asymmetry ratios on the load capacity, end slip and strain development. The load vs mid-span deflection and end-slip relationships clearly indicated that as the asymmetry ratio increased the neutral axis moved towards the bottom flange and the load capacity increased. However, when the asymmetry ratio reached 3.5, it appears

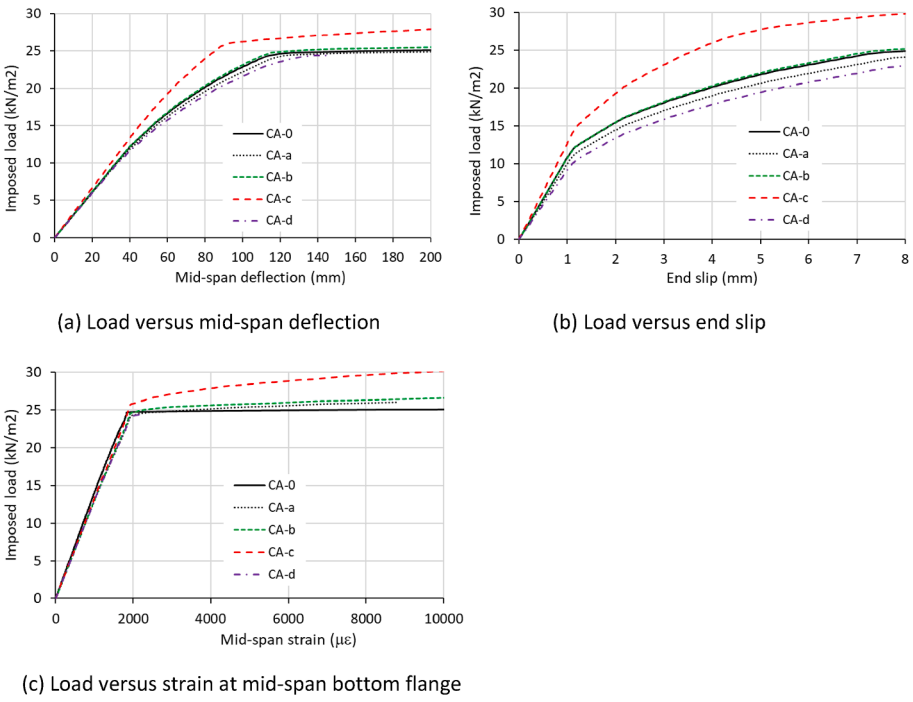

Fig. 12. Effect of different shear connector arrangements.

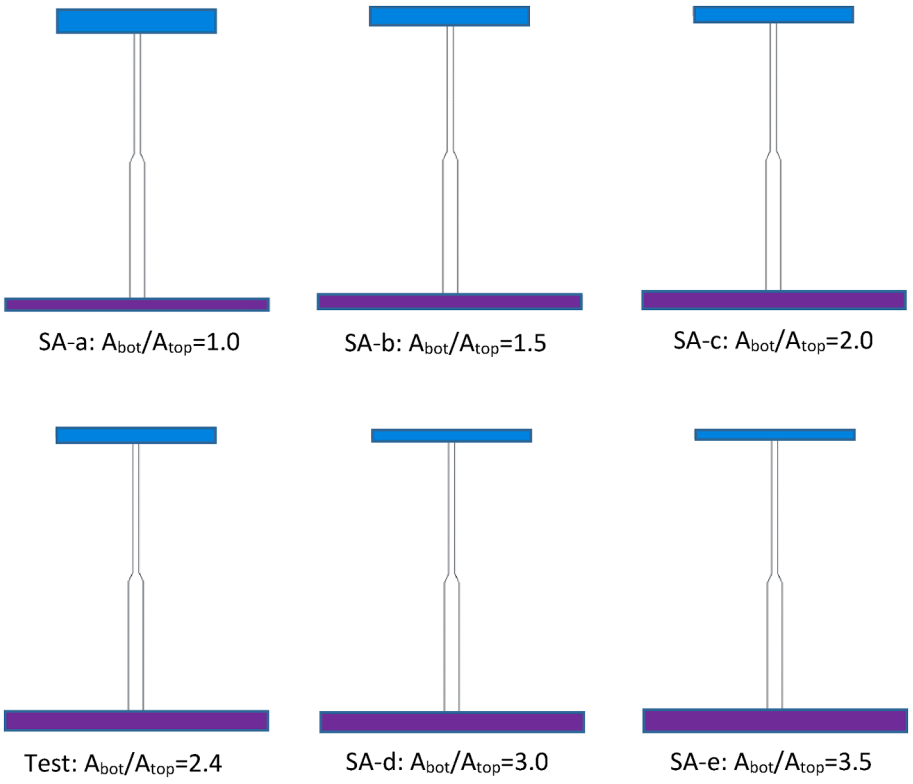

Fig. 13. Six different steel beam sectional asymmetry ratios adopted in the parametric study.

that the bearing capacity decreased slightly compared with the ratio of 3.0. This is due to the failures of the top flange and connection as the thickness is less than 9 mm. For an asymmetry ratio of 3.5, It can be seen that when the mid-span deflection exceeded 120 mm, the end slip reached 9.5 mm, this exceeds the maximum shear connector capacity slip range 6–8.5 mm. The ABAQUS simulation automatically terminated with no yielding observed at the steel beam bottom flange but the strain developed quickly as shown in Fig. 14 (c, d) load vs strain relationships. These figures also clearly show that increasing the bottom flange area increased the load capacity of the composite beam system if the top flange meets the section classification requirement.

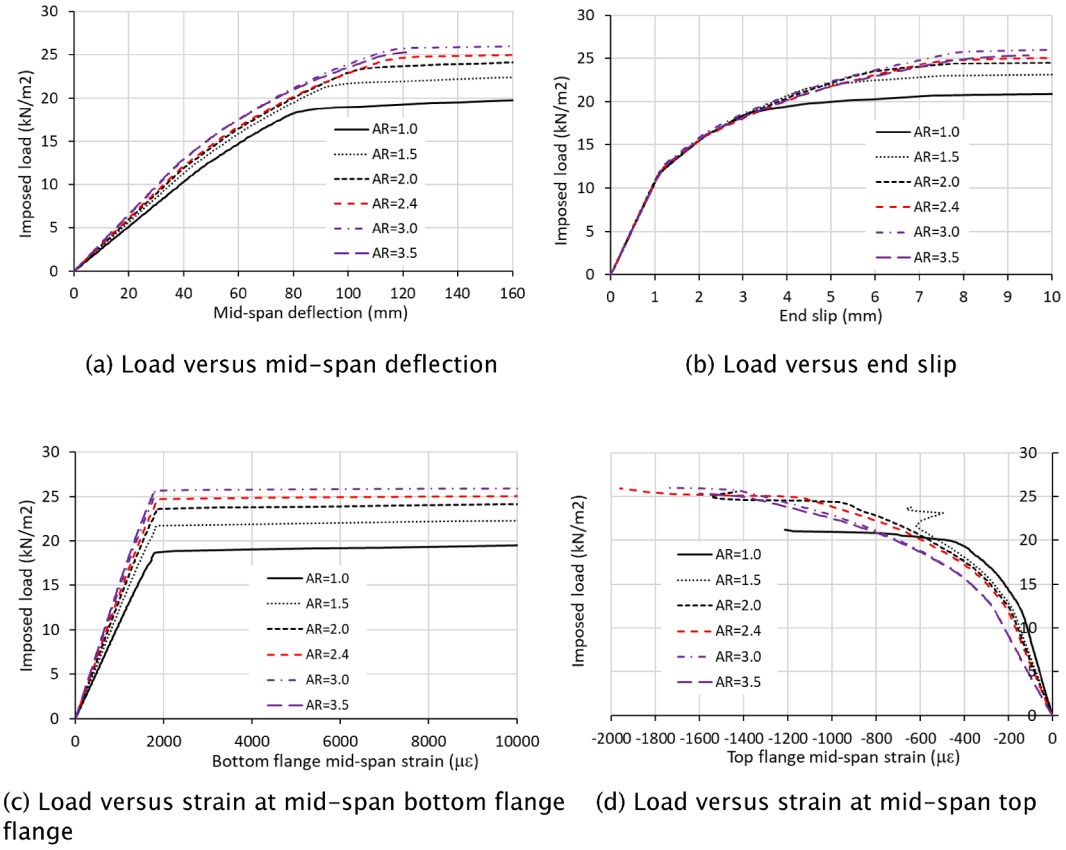

Fig. 14. Effect of beam sectional asymmetry ratios.

Table 1
Summary of main composite cellular beam design features.

Beam overall length	11.600 m	Beam span (support span) length	11.200 m
Overall depth	427.2 mm	Design beam spacing	2.800 m
Cells (openings) data			
Centre diameter	300 mm	Centre spacing	450 mm
Number of cells in beam	25	Number of cells with infill	6
Top Tee		**Bottom Tee**	
Tee depth	211.7 mm	Tee depth	215.3 mm
Tee depth at centreline of opening	61.7 mm	Tee depth at centreline of opening	65.3 mm
Web thickness	6.7 mm	Web thickness	9.9 mm
Flange width	165.7 mm	Flange width	306.3 mm
Flange thickness	11.8 mm	Flange thickness	15.4 mm
Root radius	8.9 mm	Root radius	15.2 mm
Steel yield strength (by test)	394.0 N/mm2	Steel yield strength (by test)	410.0 N/mm2
Decking data: ComFlor 80			
Sheet thickness	0.9 mm	Design strength	450 N/mm2
Slab data			
Overall depth	150 mm	Concrete strength (cubic, by test)	40 N/mm2
Reinforcement mesh			
Type	A193	Design strength	500 N/mm2

4. Simple prediction methods for plastic moment

4.1. Simple calculation methods by SCI

For a composite beam with unstiffened web opening, direction calculation method for plastic bending moment resistance at the centreline of the opening, $M_{o,Rd}$, can be found in the Chapter 3 in SCI publication P355 [38], in which two situations, (1) the compression resistance of the full depth of the effective width of slab is greater than the tension resistance of the bottom Tee and (2) the compression resistance of the full depth of the effective width of slab is less than the tension resistance of the bottom Tee, may be considered. Detailed information is documented in Section 3.2.2 in SCI publication P355 and omitted here for clarity.

For the first situation, it is considered that the plastic neutral axis is within the slab at a height such that all the concrete above it develops a stress of $0.85f_{cd}$ (where f_{cd} is the concrete design strength, is as defined in BS EN 1994-1-1). The plastic bending resistance at the centreline of the opening is then given by:

$$M_{o,Rd} = N_{bT,Rd}\left(h_{eff} + z_t + h_s - 0.5z_c\right) \quad (1)$$

Where,h_{eff} is the effective depth of the beam between the centroids of the top Tee and bottom Tee,z_t is the depth of the centroid of the top Tee from the outer edge of the flange,h_s is the slab depth,z_c is the depth of concrete in compression, which is calculated by:

$$z_c = \frac{N_{c,Rd}}{0.85f_{cd}b_{eff,o}} \le h_c \quad (2)$$

$$N_{c,Rd} = min\left\{0.85f_{cd}b_{eff,o}h_c; n_{sc}P_{Rd}\right\} \quad (3)$$

Where,f_{cd} is the design strength of the concrete ($=\frac{f_{ck}}{\gamma_c}$, with f_{ck} and γ_c as defined in BS EN 1992-1-1 [36] and its National Annex),$b_{eff,o}$ is the effective slab width at the opening,h_c is the depth of the concrete topping ($h_c = h_s - h_d$).h_d is the overall depth of the decking profile,n_{sc} is the number of the shear connectors placed over the distance from the nearer support to the centerline of the opening (here, is the number of shear connectors from support to the mid-span),P_{Rd} is the design resistance of the shear connectors used with profiled sheeting,$N_{bT,Rd}$ is the tensile

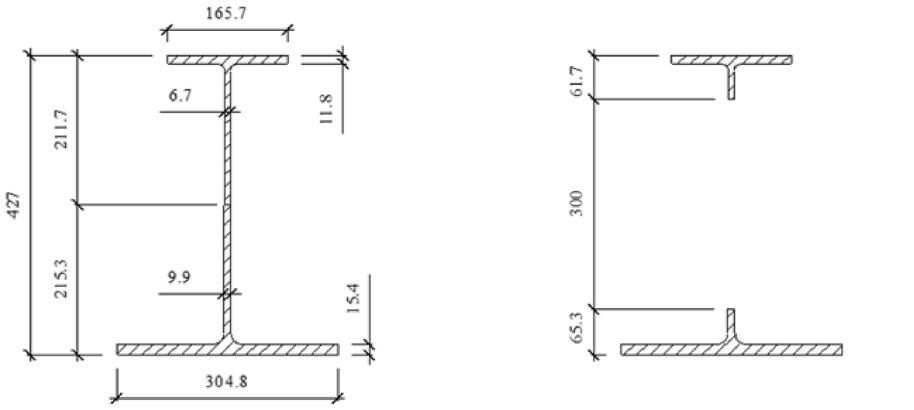

(a) Solid section (b) Section at centreline of opening

Fig. 15. Steel beam cross sectional dimensions.

Table 2
Moment resistance of composite beams with different concrete strengths.

Concrete grades	C20	C30	C32 (test)	C40	C50	C60
Concrete cylinder strength f_{ck} (N/mm2)	20	30	32	40	50	60
Mid-span plastic moment (PM) resistance by SCI method: $M_{o,Rd,SCI}$ (kNm)	1024	1056	1061	1077	1096	1119
Mid-span deflection corresponding PM by FE modelling (mm)	–	112.5	111.5	104.8	99.0	95.0
End slip corresponding PM by FE modelling (mm)	–	7.1	7.0	5.9	4.9	4.0

Note: "–" In the modelling, the maximum mid-span moment couldn't reach the mid-span plastic moment predicted by SCI method due to the failure of concrete and shear connection, so no mid-span deflection and end slip corresponding to the predicted plastic moment.

resistance of the bottom Tee, which is given by,

$$N_{bT,Rd} = \frac{A_{bT} f_y}{\gamma_{M0}} \tag{4}$$

Where,A_{bT} is the cross sectional area of the bottom Tee,f_y is the design value of the yield strength of steel,γ_{M0} is the partial factor for resistance of steel cross sections,

For the situation where the compression resistance of the full depth of the effective width of slab is less than the tension resistance of the bottom Tee, it is conservative to assume that that top Tee is uniformly stressed and subjected to a force equal to the difference between the tension resistance of the bottom Tee and the compression resistance of the slab, i.e. it provides a resistance of $N_{bT,Rd} - N_{c,Rd}$. The plastic bending resistance is then given by:

$$M_{o,Rd} = N_{bT,Rd} h_{eff} + N_{c,Rd}(z_t + h_s - 0.5h_c) \tag{5}$$

All variables in the equation (5) are defined as previous. It is suggested to verify that for highly asymmetric sections, the compression resistance of the top Tee is adequate, as follows:

$$\frac{A_{tT} f_y}{\gamma_{M0}} \geq N_{bT,Rd} - N_{c,Rd} \tag{6}$$

A_{tT} is the cross-sectional area of top Tee.

The above direction method is adopted for composite beam with unstiffened web opening and welded shear connectors. For a composite beam with bolted shear connectors (demountable shear connectors), SCI publication P428 [2] suggests a reduction factor, k_{flex}, which is introduced to consider the "equivalent" idealised plastic behaviour for bolted shear connectors, or $k_{flex} = 0.8$ for uniform spacing bolted shear

Table 3
Moment resistance of composite beams with different shear connector arrangements.

Connector arrangement	CA-0 (test)	CA-a	CA-b	CA-c	CA-d
Number of connectors to mid-span (n_{sc})	20	20	22	38	21
Mid-span plastic moment (PM) resistance by SCI method: $M_{o,Rd,SCI}$ (kNm)	1061	1061	1076	1192	1068
Mid-span deflection corresponding PM by FE modelling (mm)	111.5	118.5	111.7	147.0	134.5
End slip corresponding PM by FE modelling (mm)	7.0	8.1	7.0	4.6	10.6

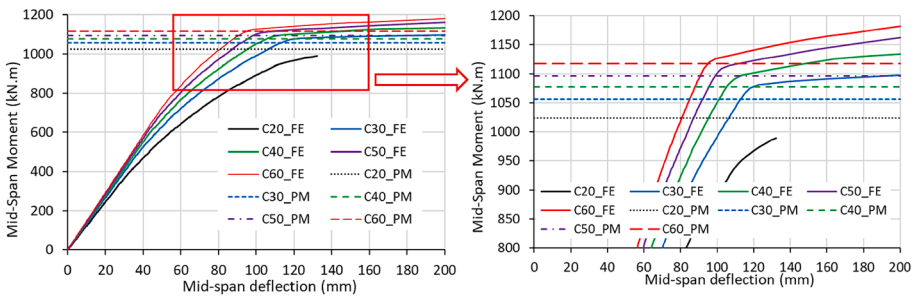

(a) Overall views (b) Enlarged views

Fig. 16. Moment resistance of composite beams with different concrete grades.

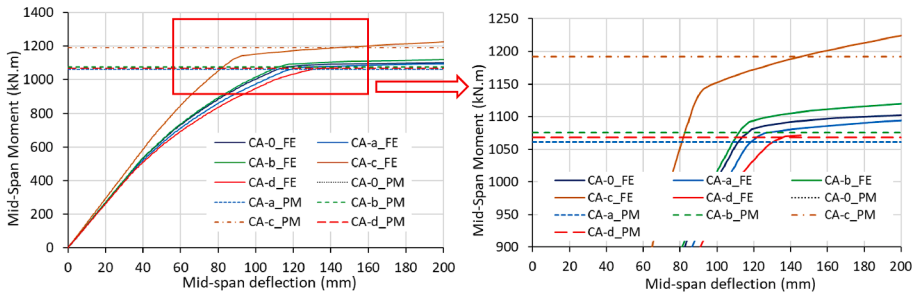

(a) Overall views (b) Enlarged views

Fig. 17. Moment resistance of composite beams with different shear connector arrangements.

Table 4
Moment resistance of composite beams with different beam flange asymmetry ratios.

Steel beam flange asymmetry ratios	1.0 (SA-a)	1.5 (SA-b)	2.0 (SA-c)	2.4 (test)	3.0 (SA-d)	3.5 (SA-e)
Top Tee flange thickness (mm)	20.06	16.05	13.38	11.80	10.03	8.92
Bottom Tee flange thickness (mm)	10.91	13.09	14.54	15.40	16.36	16.97
Mid-span plastic moment (PM) resistance by SCI method: $M_{o,Rd,SCI}$ (kNm)	833	944	1017	1061	1109	1139
Mid-span deflection corresponding PM by FE modelling (mm)	103.7	95.5	102.8	111.5	112.0	–
End slip corresponding PM by FE modelling (mm)	3.5	4.4	5.7	7.0	7.5	–

Note: "–" In the modelling, the maximum mid-span moment did not reach the mid-span plastic moment predicted by the SCI method due to the failure of the top flange. Therefore, the mid-span deflection and end slip corresponding to the predicted plastic moment were not obtained.

connector arrangement, $k_{flex} = 0.85$ for pseudo-elastic distribution bolted shear connector arrangement. For welded studs, $k_{flex} = 1.00$, if this factor is to be considered. Therefore, with the introduction of the reduction factor, the design resistance of shear connector P_{Rd} for composite beams using bolted shear connectors is $P_{Rd,eff} = k_{flex}P_{Rd}$.

The above direction method is employed to predict the plastic bending moment resistance at the mid-span opening of the tested composite beam and composite beams adopted in the parametric study. Table 1 and Fig. 15 summarises the main features of the tested composite beam. Composite beams used in the parametric study are similar to the tested beam, but slab concrete strengths, shear connector arrangements and ratios of bottom tee to top tee flange areas are parameters considered in order to explore their effects on the structural behaviour.

4.2. Composite beams with different slab concrete strengths

The SCI direction method was adopted to predict the plastic bending moment at the mid-span for 5 composite beams with different concrete strengths used in the parameter study. For different concrete grades, the maximum connector resistance P_{Rmax} are taken from Fig. 8. The design resistance of shear connector $P_{Rd} = 0.9P_{Rmax}$. The equivalent connector resistance $P_{Rd,eff} = k_{flex}P_{Rd}$, $k_{flex} = 0.85$ as the shear connector distribution is not uniform. Table 2 and Fig. 16 show the mid-span plastic moment resistance predicted by the SCI method and moment-mid-span relationship predicted by FE modelling for composite beams with different concrete strengths, respectively. It can be seen that, for concrete strength of 30 N/mm^2 or over, the predicted plastic moment resistance is close to (just slightly lower than) the moment from the FE model results, but for slab concrete strength of 20 N/mm^2, the predicted plastic moment resistance is higher than the maximum moment obtained from FE model prediction due to the failure of concrete and shear connection. The comparison indicated that the SCI direction method may be conservative for composite beams with higher strength concrete but may overestimate the capacity of composite beams with low concrete grades.

4.3. Composite beams with different shear connector arrangements

As shown in the parameter study of composite beams with different shear connector arrangements, when using the SCI direction method to predict the mid-span plastic moment resistance, the composite beams adopted are the same as the tested composite beam (CA-0) but the shear connector arrangements are different as shown in Fig. 11 to consider the effect. The concrete cylinder strength 32 N/mm^2 was taken for all cases, therefore the maximum connector resistance is $P_{Rmax} = 75$ kN as shown in Fig. 5. The design resistance of shear connector $P_{Rd} = 0.9P_{Rmax}$. The equivalent connector resistance $P_{Rd,eff} = k_{flex}P_{Rd}$, $k_{flex} = 0.80 or 0.85$ for uniform spacing and pseudo-elastic distribution respectively. It must be noted that the number of shear connectors (n_{sc}) from the end support to the mid-span for each specimen are different from that of tested specimen CA-0 except for CA-a, whose shear connector number is the same. Table 3 and Fig. 17 show the mid-span plastic moment resistance predicted by the SCI method and the mid-span moment to mid-span deflection relationship predicted by FE modelling for composite beams with different shear connector arrangements. It can be seen that the mid-span plastic moment predicted by the SCI method clearly reflected the effect of using different numbers of shear connectors. But for specimens with arrangement patterns such as those of CA-0 and CA-a, their plastic moments are almost the same, but the FE modelling reflected the effect of the shear connector arrangements and the shear connector number. CA-0 possesses a higher resistance due to more connectors being arranged close to the end support (comparison of CA-0 and CA-a). The predicted plastic moment resistance by the SCI method is very close to moments from the tests and modelling. For shear connector spacing with pseudo-elastic distribution, generally the predicted plastic moment resistance is close to (slightly low than) the moment from the FE model results, the SCI method appears conservative for cases with more shear connectors adopted close to the end of the beam. For shear connector spacing with uniform spacing distribution (CA-c), the predicted plastic moment resistance appears to be overestimated by the FE model.

4.4. Composite beams with different flange asymmetry ratios

In the parametric study for composite beams with different asymmetry ratios, as shown in Fig. 13 and Table 4, the thicknesses of the top flange and bottom flange changed, but the breadths of the top and bottom flanges are the same as the tested specimen, 165.7 mm and

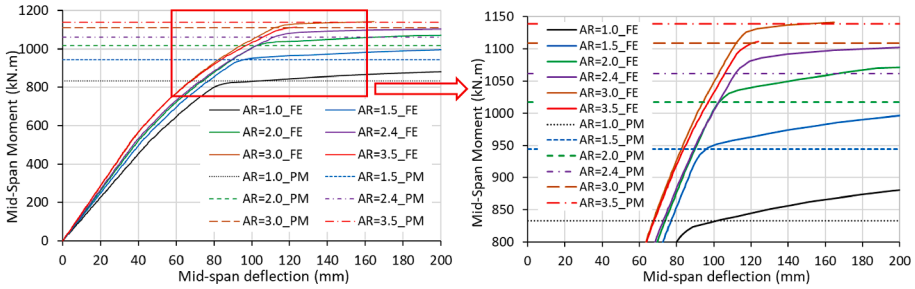

(a) Overall views (b) Enlarged views

Fig. 18. Moment resistance of composite beams with different beam flange asymmetry ratios.

304.8 mm respectively. In addition, no change has been introduced to the web thicknesses and depths, therefore all beams have the same cross-sectional areas. The concrete cylinder strength is 32 N/mm^2, the same as the tested composite beam, therefore the maximum connector resistance P_{Rmax} = 75 kN as shown in Fig. 5. The design resistance of shear connector $P_{Rd} = 0.9P_{Rmax}$. The equivalent connector resistance $P_{Rd,eff} = k_{flex}P_{Rd}$. Taking $k_{flex} = 0.85$ to consider connectors are bolted shear connectors with non-uniform spacing. Table 4 and Fig. 18 show the mid-span plastic moment resistances predicted by SCI method and mid-span moment and mid-span deflection relationships predicted by FE modelling. Due to poor convergence, the model with AR = 3.5_FE aborted earlier. But this did not impact significantly in terms of interpreting the results. It can be seen, for an asymmetry ratio not exceeding 3.0, that the mid-span plastic moments predicted by SCI method are close to the mid-span moments predicted by the FE models where the composite beams experienced decreasing stiffness afterwards or just before (asymmetry ratio 1.0). For an asymmetry ratio greater than 3.0, such as 3.5, the mid-span plastic moment predicted by the SCI method is higher than the maximum mid-span moment from the FE modelling result due to the top flange thickness being too small and not meeting the section classification requirement, so the SCI direction method can't be used.

5. Conclusions

Following the experimental study of a cellular steel concrete composite beam, a FE model was developed using ABAQUS software and validated against the experimental observation. Satisfactory agreement was obtained. The comparison and analysis indicated that the FE model developed using ABAQUS software could be used to capture the structural behaviour of this kind of composite beam including load bearing capacity, deflection, slip behaviour, stress/strain development and failure mode. Following the validation of the modelling method, a parametric study, covering different slab concrete strengths, different demountable shear connector arrangements and different asymmetry ratios of the steel beam section, was conducted. The parametric study further highlighted the structural behaviour and performance of the composite cellular beam system. Finally, the SCI direction method was adopted to predict the mid-span plastic moment resistance of composite beams with different concrete strengths, shear connector arrangements and section asymmetry ratios and compared with mid-span moments obtained from FE modelling, good agreement can be seen. The following conclusions can be drawn according to the numerical analysis:

(a) the higher the concrete strength, the higher the composite beam stiffness and load capacity. However, for lower slab concrete strength, such as C20/25, the steel section might not develop its full loading capacity due to the shear connector failure, thus for the chosen steel section, it is recommended that the slab concrete grade shall not be lower than C30/37;
(b) the arrangement of the shear connectors affected the behaviour of composite beam. The shear connectors close to the beam end contribute more shear resistance to the composite beam system due to the occurrence of higher slip close to ends and thus pairs of connectors are recommended;
(c) the increase of the asymmetry ratio resulted in the neutral axis moving downwards and an increase in the composite beam stiffness or loading capacity. However, when the asymmetry ratio was 3.5, due to the small thickness of top flange, it appears that earlier shear connector failure reduced the loading capacity of the composite beam system. It is recommended, for the chosen beam section and adopted concrete grade, that an asymmetry ratio of 2.0 – 3.0 be adopted.
(d) the SCI direction method may be used to predict the plastic bending moment resistance of cellular composite beams using bolted/demountable shear connectors.

Declaration of Competing Interest

The authors declare that they have no known competing financial interests or personal relationships that could have appeared to influence the work reported in this paper.

Acknowledgement

The research leading to these results is part of a joint project of the University of Bradford, the University of Luxemburg, the Technology University of Delft, the Steel Construction Institute, Tata Steel, Lindab S. A., BmS and AEC3 Ltd. The authors gratefully acknowledge the funding received from the European Commission: Research Fund for Coal and Steel (RFCS-2015, RPJ, 710040). In addition, deep appreciation to Mr. Stephen Robinson for his work done in the laboratory.

References

[1] Global Alliance for Buildings and Construction, International Energy Agency and the United Nations Environment Programme (2019): 2019 global status report for buildings and construction: Towards a zero-emission, efficient and resilient buildings and construction sector.
[2] Girão AM, Coelho ML, Lam D, Yang J. Guidance on demountable composite construction systems for UK practice (SCI P428). Ascot, UK: The Steel Construction Institute; 2020.
[3] Katwal U, Tao Z, Hassan M, Uy B, Lam D. Load sharing mechanism between shear studs and profiled steel sheeting in push tests. J Constr Steel Res 2020;174:106279.
[4] Mark Lawson R, Anthony Saverirajan AH. Simplified elasto-plastic analysis of composite beams and cellular beams to Eurocode 4. J Constr Steel Res 2011;67 (10):1426–34.
[5] Moynihan MC, Allwood JM. Viability and performance of demountable composite connectors. J Constr Steel Res 2014;99:47–56.
[6] Sheehan T, Dai X, Lam D, Aggelopoulos E, Lawson M, Obiala R. Experimental study on long spanning composite cellular beam under flexure and shear. J Constr Steel Res 2016;116:40–54.
[7] Wang J-Y, Guo J-Y, Jia L-J, Chen S-M, Dong Y. Push-out tests of demountable headed stud shear connectors in steel-UHPC composite structures. Compos Struct 2017;170:69–79.
[8] Yang F, Liu Y, Jiang Z, Xin H. Shear performance of a novel demountable steel-concrete bolted connector under static push-out tests. Eng Struct 2018;160:133–46.

[9] Lawson RM, Lam D, Aggelopoulos E, Hanus F. Serviceability performance of composite cellular beams with partial shear connection. J Constr Steel Res 2018; 150:491–504.
[10] Kozma A, Odenbreit C, Braun MV, Veljkovic M, Nijgh MP. Push-out tests on demountable shear connectors of steel-concrete composite structures. Structures 2019;21:45–54.
[11] Sheehan T, Dai X, Yang J, Zhou K, Lam D. Flexural behaviour of composite slim floor beams. Structures 2019;21:22–32.
[12] Suwaed ASH, Karavasilis TL. Demountable steel-concrete composite beam with full-interaction and low degree of shear connection. J Constr Steel Res 2020;171: 106152.
[13] Nijgh MP, Veljkovic M. An optimisation strategy for the (in- and out-of-plane) resistance of steel beams in demountable composite floor systems. Structures 2020; 24:880–9.
[14] Dai X, Lam D, Sheehan T, Yang J, Zhou K. Effect of Dowel Shear Connector to Performance of Slim-Floor Composite Shear Beams. J Constr Steel Res 2020;173: 106243.
[15] Qureshi J, Lam D, Ye J. Effect of shear connector spacing and layout on the shear connector capacity in composite beams. J Constr Steel Res 2011;67:706–19.
[16] Qureshi J, Lam D, Ye J. The influence of profiled sheeting thickness and shear connector's position on strength and ductility of headed shear connector. Eng Struct 2011;33:1643–56.
[17] Felipe Piana Vendramell Ferreira, Konstantinos Daniel Tsavdaridis, Carlos Humberto Martins, Silvana De Nardin (2021), "Ultimate strength prediction of steel–concrete composite cellular beams with PCHCS", Engineering Structures, Vol 236, 112082.
[18] Csillag F, Pavlović M. Push-out behaviour of demountable injected vs. blind-bolted connectors in FRP decks. Compos Struct 2021;Vol 270,114043.
[19] Wen J, Sheikh A, Uddin M, Uy B. Analytical model for flexural response of two-layered composite beams with interfacial shear slip using a higher order beam theory. Compos Struct 2018;184:789–99.
[20] Xianghe Dai, Jie Yang, Dennis Lam, Therese Sheehan, Kan Zhou (2022), "Experiment and numerical modelling of a demountable steel connection system for reuse", J Constr Steel Res, Vol 198, 107534.
[21] He J, Suwaed ASH, Vasdravellis G, Wang S. Behaviour and design of the 'lockbolt' demountable shear connector for sustainable steel-concrete structures. Structures 2022;44:988–1010.
[22] D. Lam X. Dai E. Saveri Behaviour of Demountable Shear Connectors in Steel-Concrete Composite Beams 2013 North Queensland, Australia.
[23] Lam D, Dai X, Ashour A, Rehman N. Behaviour of demountable shear connectors in composite beams with profiled deck flooring. Eighth International Conference on Advances in Steel Structures. 2015.
[24] Dai X, Lam D, Saveri E. Effect of Concrete Strength and Stud Collar Size to Shear Capacity of Demountable Shear Connectors. J Struct Eng (ASCE) 2015.
[25] Rehman N, Lam D, Dai X, Ashour AF. Experimental study on demountable shear connectors in composite slabs with profiled decking. J Constr Steel Res 2016;122: 178–89.
[26] Dennis Lam, Xianghe Dai, Ashraf Ashour, Naveed Rahman (2017). "Recent research on composite beams with demountable shear connectors". Steel Construction 10 (2017), No. 2.
[27] Use of bolted shear connectors in composite construction X. Dai D. Lam T. Sheehan J. Yang K. Zhou Proceedings of the 12th International Conference on Advances in Steel-Concrete Composite Structures 2018 475 482.
[28] Yang J, Lam D, Dai X, Sheehan T. Experimental study on demountable shear connectors in profiled composite slabs. In: Proceedings of the 12th International Conference on Advances in Steel-Concrete Composite Structures; 2018. p. 115–21.
[29] Dennis Lam, Jie Yang, Xianghe Dai, Therese Sheehan and Kan Zhou (2018), "Design Composite Structures for Reuse". Ninth International Conference on Advances in Steel Structures (ICASS'2018), 5-7 December 2018 - Hong Kong, China.
[30] D. Lam T. Sheehan X. Dai Innovative flooring system for steel-concrete composite construction 2018 Perth, Australia 31st Jan – 2nd Feburary.
[31] Naveed Rahman, Dennis Lam, Xianghe Dai, Ashraf Ashour (2018). "Testing of composite beam with demountable shear connectors". *Structures and Buildings* Volume 171 Issue SB1, 3-16. Proceedings of the Institution of Civil Engineers. ISSN 0965-0911 | E-ISSN 1751-7702.
[32] Push tests on demountable shear connectors in profiled composite slabs J. Yang D. Lam X. Dai T. Sheehan K. Zhou Y.C. Wang R.M. Sencu The 2019 World Congress on Advances in Structural Engineering and Mechanics (ASEM19) Jeju Island 2019.
[33] Lam D, Yang J, Dai X, Sheehan T, Zhou K. Development of Composite Floor System for a Circular Economy. The 2019 World Congress on Advances in Structural Engineering and Mechanics (ASEM19) Jeju Island. 2019.
[34] Sheehan T, Yang J, Lam D, Dai X, Zhou K. Experimental Study of Composite Steel Cellular Beam System Using Demountable Shear Connectors. The 9th European Conference on Steel and Composite Structures. 2021.
[35] Lam D, Yang J, Wang Y, Dai X, Sheehan T, Zhou K. New composite flooring system for the circular economy. Steel Compos Struct 2021;40(5):649–61.
[36] EN1992-1-1: Eurocode 2 – Design of concrete structures - Part 1-1: General rules and rules for buildings. Brussels, Belgium: European Committee for Standardization (CEN); 2004.
[37] EN1994-1-1: Eurocode 4 – Design of composite steel and concrete structures. Part 1-1: General rules and rules for buildings. Brussels, Belgium: European Committee for Standardization (CEN); 2004.
[38] Lawson M, Hicks SJ. Design of composite beams with large web openings (SCI P355). Ascot, UK: The Steel Construction Institute; 2011.